RSC Advances

PAPER

Check for updates

Synergetic effect of Na-doping and carbon coating on the electrochemical performances of Li₃₋ₓNaₓV₂(PO₄)₃/C as cathode for lithium-ion batteries

Xuedong Yan,[a] Liqing Xin,[b] Hang Wang, [ID] *[c] Changhe Cao[de] and Shanshan Sun[de]

Carbon coated $Li_{3-x}Na_xV_2(PO_4)_3$/C (x = 0.04, 0.06, 0.10, 0.12, 0.18) cathode materials for lithium-ion batteries were synthesized *via* a simple carbothermal reduction reaction route using methyl orange as the reducing agent, which also acted as the Na and carbon sources. The influence of various Na-doping levels on the structure and electrochemical performance of the $Li_{3-x}Na_xV_2(PO_4)_3$/C composites was investigated. The valence state of vanadium, the form of residual carbon and the overall morphology of the $Li_{2.90}Na_{0.10}V_2(PO_4)_3$/C, which showed the highest initial specific discharge capacity of 128 mA h g^{-1} at the current density of 0.1C (1C = 132 mA g^{-1}) among this series of composites, were further examined by X-ray photoelectron spectroscopy, Raman spectroscopy, scanning electron microscopy and high-resolution transmission electron microscopy, respectively. The results indicated that a well crystallized structure of Na-doped $Li_{2.90}Na_{0.10}V_2(PO_4)_3$ coated by a carbon matrix is obtained. In the further electrochemical measurements, the $Li_{2.90}Na_{0.10}V_2(PO_4)_3$/C cathode material shows superior discharge capacities of 124, 118, 113, 106 and 98 mA h g^{-1} at 0.3, 0.5, 1, 2 and 5C, respectively. High capacity retention of 97% was obtained after 1100 cycles in long-term cyclic performance tests at 5C. The reason for such a promising electrochemical performance of the as-prepared $Li_{2.90}Na_{0.10}V_2(PO_4)_3$/C has also been explored, which revealed that the synergetic effect of the Na-doping and carbon coating provide enlarged Li$^+$ diffusion channels and the increased electronic conductivity.

1. Introduction

For new large-scale applications such as electric vehicles (EVs), hybrid electric vehicles (HEVs), and power backup, the rechargeable lithium-ion batteries (LIBs) should offer both long-term cyclic stability and high rate capability. Novel cathode materials based on metallic lithium phosphates such as $LiMPO_4$ (M = Fe, Co, Ni, Mn)[1–5] and $Li_3M_2(PO_4)_3$ (M = Fe, V)[6–13] are promising cathodes for large-scale LIBs due to their superior thermal stability and cyclic performance. Recently, monocline $Li_3V_2(PO_4)_3$ cathode materials have attracted particular interest due to their unique advantages, such as high operation voltage, theoretical specific capacity and ion mobility as well as excellent thermal stability.[7–11] However, monocline $Li_3V_2(PO_4)_3$ suffers from the intrinsic disadvantage of poor electronic conductivity

[a] College of Chemical Engineering, Ningbo Polytechnic, Ningbo 315800, PR China
[b] School of Metallurgy and Environment, Central South University, Changsha 410000, PR China
[c] College of Electronics and Computer Science, Zhejiang Wanli University, No. 8 Qianhunan Road, Ningbo 315100, PR China. E-mail: 48230200@qq.com; Tel: +86-137-7705-0597
[d] Ningbo Veken New Energy Technology Limit Corporation, Ningbo 315800, P. R. China
[e] Ningbo Veken Technology Research Institute, Ningbo 315800, P. R. China

(ca. 2.3×10^{-8} S cm^{-1} at 300 K),[11] which limits its applications in large-scale energy storage devices.

To address the aforementioned challenges, different methods, such as metal ion doping[10,14–19] and carbon coating[20–28] have been adopted. Among them, carbon which can be *in situ* formed by the decomposition of organic precursor serving as a surface coating of the particles can suppress the growth of grain to reduce the particle size and enhance the electronic conductivity of $Li_3V_2(PO_4)_3$.[19,22,23,25–27] Based on this, the carbon plays an irreplaceable role in improving rate capability and cyclic retention of $Li_3V_2(PO_4)_3$ cathode materials. On the other hand, various metallic cations are chosen to substitute the V-site or Li-site in $Li_3V_2(PO_4)_3$ phase.[29–34] In the case of V-site substitution, although the bulk electronic conductivity of $Li_3V_{2-y}M_y(PO_4)_3$ is enhanced, the potential plateaus become more slopping because of the different electrochemical activities between V^{3+} and other metallic cations (Ti^{4+}, Zr^{4+}, Cr^{3+}, Mg^{2+}, Co^{2+}, et. al.).[17–19] Compared with the V-site doping, the Li-site doping of $Li_3V_2(PO_4)_3$ can not only maintain the potential plateaus during cycling, but also increase the bulk electronic conductivity and enlarge the diffusion channel of Li$^+$. For examples, the rate capability and cyclic retention of Na-doped $Li_{3-x}Na_xV_2(PO_4)_3$ cathode materials are obviously

enhanced.[32–34] Nevertheless, only limited cyclic performance (<100 cycles) under moderate rates (≤2C) were reported[32–34] In addition, sol–gel method and rheological phase reaction method were the common methods chosen to prepare Na-doped $Li_3V_2(PO_4)_3$,[32–34] however, these methods are not suitable for large-scale production compared to the solid-state reaction method because of their complex manufacturing process and time consuming. Moreover, as the doping amount of Na in $Li_3V_2(PO_4)_3$ required a low level, the commonly used inorganic Na sources of Na_2CO_3,[32] $NaNO_3$,[33] Na_3PO_4 (ref. 34) in the synthesis of Na-doped $Li_3V_2(PO_4)_3$ are hardly to achieve homogeneously Na distributed Na-doped $Li_3V_2(PO_4)_3$ via solid-state reaction method as only a little volume of these Na sources is needed due to the large bulk density of inorganic compounds ($V = m/\rho$, m is the needed mass of Na source, ρ is the bulk density of Na source, and V is the needed volume of Na source).

Herein, a series of Na-doped $Li_{3-x}Na_xV_2(PO_4)_3$/C ($x = 0.04$, 0.06, 0.10, 0.12, 0.18) cathode materials with carbon coating were synthesized via a simple carbothermal reduction reaction (CTR) synthetic strategy using methyl orange as both reduction agent and Na and carbon sources. Among them, $Li_{2.90}Na_{0.10}V_2(PO_4)_3$/C composite shows superior physical properties on crystalline structure, carbon matrix, and electronic conductivity which help enhancing its electrochemical performances. The $Li_{2.90}Na_{0.10}V_2(PO_4)_3$/C composite provides a long-term cyclic stability. Capacity retention of 97% is obtained after 1100 cycles at the current density of 5C. To the best of our knowledge, long-term cyclic performance over 500 cycles especially at 5C of Na-doped $Li_{3-x}Na_xV_2(PO_4)_3$/C cathode is not reported previously.

2. Experimental

Carbon coated $Li_{3-x}Na_xV_2(PO_4)_3$/C ($x = 0.04$, 0.06, 0.10, 0.12, 0.18) composites with different amounts of Na-doping were synthesized by a solid-state reaction route. Typically, methyl orange was used as both reduction agent and Na and carbon sources, in which LiH_2PO_4 (AR, 99.9%) and V_2O_5 (AR, 99.9%) were used to synthesized original $Li_3NaV_2(PO_4)_3$. Stoichiometric raw materials based on the chemical formula of $Li_3NaV_2(PO_4)_3$ were mixed in ethanol and ball milled for 5 h by using zirconia balls. Then, the mixed slurry was dried in an oven at 60 °C for 12 h followed by an annealing process at 300 °C for 1 h under nitrogen. After being calcined at 850 °C for 8 h, $Li_{3-x}Na_xV_2(PO_4)_3$/C sample were obtained.

The crystal structure of the $Li_{3-x}Na_xV_2(PO_4)_3$/C composites was detected by X-ray diffraction (XRD, Rigaku P/max 2200VPC) using Cu Kα radiation. The chemical valence state of V in the $Li_{3-x}Na_xV_2(PO_4)_3$/C composite was determined by X-ray photoelectron spectroscopy (XPS) using Thermo ESCALAB 250 spectrometer with monochromatic Al Kα radiation. Resonant Raman scattering spectra were recorded at room temperature with a JY HR-800 Lab Ram confocal Raman microscope with an excitation wavelength of 325 nm. The microstructure of the composites was observed using scanning electron microscopy (SEM, XL 30 ESEM-FEG, FEI Company) and high resolution transmission electron microscopy (HRTEM, JEM-2010). For the

measurement of electronic conductivity, powder sample was pressed in disks of 15 mm in diameter and 2 mm in thickness using a four-point probe meter (SDY-5, Guangzhou). The carbon contents in $Li_{3-x}Na_xV_2(PO_4)_3$/C composites were determined by the VarioEL III (elementar, Germany) element analyzer.

The electrochemical performances of the $Li_{3-x}Na_xV_2(PO_4)_3$/C composites as cathode for LIBs were evaluated using a coin-type 2025 cell using metallic lithium as anode, in which the electrodes were produced by spreading a slurry mixed by 84 wt% active materials ($Li_{3-x}Na_xV_2(PO_4)_3$/C), 8 wt% carbon black, 8 wt% polyvinylidene fluoride (PVDF) and N-methylpyrrolidone (NMP) as solvent onto an aluminum foil and dried in a vacuum oven at 120 °C for 12 h. The loading of $Li_{3-x}Na_xV_2(PO_4)_3$/C in each electrode was 2–3 mg cm^{-2}. The cells were assembled in a glove box filled with high-purity argon using anode of Li metal and separator of micro-porous polypropylene. 1 M $LiPF_6$ in a mixture of ethylene carbonate (EC) and dimethyl carbonate (DMC) (1 : 1 by volume) was used as electrolyte. The cells were galvanostatically charged and discharged between 3.0 and 4.2 V at room temperature (25 °C) on an electrochemical test instrument (CT2001A, Wuhan Land Electronic Co. Ltd., China). The capacity of the prepared cathode is calculated according the discharge capacity of the half-coin cells divided by the loading of active material.

3. Results and discussion

3.1 Structural characterization

The XRD patterns of the $Li_{3-x}Na_xV_2(PO_4)_3$/C ($x = 0.04$, 0.06, 0.10, 0.12, 0.18) composites are shown in Fig. 1, in which the sharp diffraction peaks indicate a good crystallinity for all the samples. The main diffraction peaks are well indexed to monoclinic structure with the space group of $P2_1/n$ of $Li_3V_2(PO_4)_3$ (JCPDS no. 80-1515), which are consistent with the previous reports.[35,36] The lattice parameters of Li $Li_{3-x}Na_xV_2(PO_4)_3$/C are $a = 8.4935$ Å, $b = 11.8776$ Å, $c = 8.7463$ Å, and $V = 882.64$ Å^3. The change of the lattice parameters can be the clue illustrating the doping of Na ions into the $L_3V_2(PO_4)_3$ lattice.

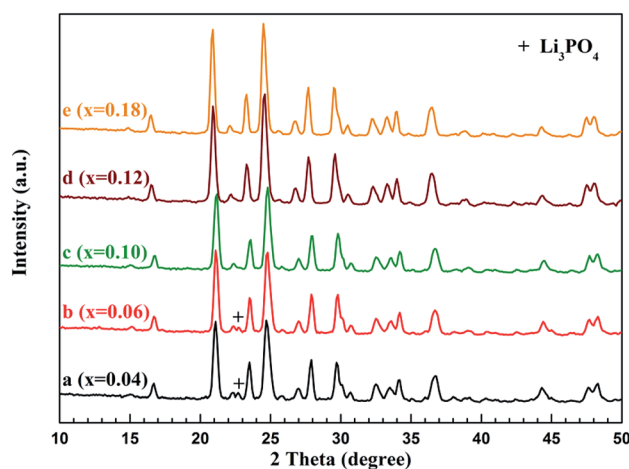Fig. 1 XRD patterns of the $Li_{3-x}Na_xV_2(PO_4)_3$/C composites. Curves a, b, c, d and e corresponding to $x = 0.04$, 0.06, 0.10, 0.12 and 0.18, respectively.

Besides, there is not any extra reflections observed for the $Li_{3-x}Na_xV_2(PO_4)_3/C$ with $x \geq 0.10$, which indicated that Na enter into the structure of $Li_{3-x}Na_xV_2(PO_4)_3/C$ rather than forming impurities.[32] However, the impurity of Li_3PO_4 corresponding the diffraction peak at 22.7° (denoted by "+") can be observed in $Li_{3-x}Na_xV_2(PO_4)_3/C$ with $x = 0.04$ and 0.06. The carbon-related diffraction peaks especially attributed to crystalline carbon are not detected in the XRD patterns, which indicates that the carbon generated from methyl orange is amorphous in a low level. Notably, high purity of $Li_{3-x}Na_xV_2(PO_4)_3/C$ composites can be synthesized when x is higher than 0.06.

Fig. 2 shows the initial galvanostatic charge–discharge curves of the $Li_{3-x}Na_xV_2(PO_4)_3/C$ as cathode for LIBs at the current density of 0.3C ($1C = 132$ mA g^{-1}) in the voltage range of 3.0 to 4.2 V. Except for the $Li_{2.82}Na_{0.18}V_2(PO_4)_3/C$, the samples exhibit three pairs of discharge–charge flat plateaus, corresponding a multi-phase transition processes occurred during the electrochemical reactions. For the $Li_{2.82}Na_{0.18}V_2(PO_4)_3/C$ composite, there is one additional charge–discharge potential plateau located at about 3.7 V (as compared to the curves of "c" and "e" in details in the inset in Fig. 2), the additional one is the characteristic charge–discharge potential plateau of the $Li_3V_2(PO_4)_3$ and $Li_2NaV_2(PO_4)_3$ with rhombohedral structure.[37,38] It has been reported that the specific capacity of the rhombohedral $Li_3V_2(PO_4)_3$ or $Li_2NaV_2(PO_4)_3$ is lower than that of the monoclinic $Li_3V_2(PO_4)_3$, although the rhombohedral structure can supply fast ion-mobility. Therefore, the presence of rhombohedral $Li_3V_2(PO_4)_3$ or $Li_2NaV_2(PO_4)_3$ is not beneficial to the capacity output of the Na-doped $Li_{3-x}Na_xV_2(PO_4)_3/C$ composite. The initial discharge specific capacities for the Na-doped $Li_{3-x}Na_xV_2(PO_4)_3/C$ composite are $ca.$ 112, 117, 124, 119, and 114 mA h g^{-1} for x of 0.04, 0.06, 0.10, 0.12 and 0.18, respectively. Discharge capacity of the composite increases firstly and then decreases with the increase of x, reaching a maximum when $x = 0.10$. It has been reported that the cell volume of $Li_3V_2(PO_4)_3$ is enlarged after the substitution of Na for Li, as the radius of Na ($r = 0.097$ nm) is larger than that of Li ($r = 0.068$ nm), which results in large channel for rapid transfer of

Li$^+$.[32–34] Methyl orange provides both Na and carbon to the $Li_{3-x}Na_xV_2(PO_4)_3/C$ composites. The carbon content for the $Li_{3-x}Na_xV_2(PO_4)_3/C$ composite detected by carbon–sulfur analyzer are $ca.$ 1.1, 1.8, 2.2, 3.2, and 4.3 wt% for x of 0.04, 0.06, 0.10, 0.12 and 0.18, respectively. The electrochemical performance of all the $Li_{3-x}Na_xV_2(PO_4)_3/C$ composites is better than that of the $Li_3V_2(PO_4)_3$ without Na doping and carbon coating reported previously.[36] As reported in literatures,[32–34] the rate performance, cyclic ability and the charge transfer property of $Li_{3-x}Na_xV_2(PO_4)_3$ composite are all enhanced after suitable Na-doping because that the Na-doping can not only enlarges the Li$^+$ diffusion channel, but also increases the bulk electronic conductivity. Moreover, in our previous report,[36] the $Li_3V_2(PO_4)_3/C$ composite exhibits significantly better electrochemical performances than the pristine $Li_3V_2(PO_4)_3$, which is attributed to the drastically increased electronic conductivity of the composite by carbon coating. Therefore, it can be concluded that it is the synergetic effect of Na-doped and carbon coating that causes the excellent charge/discharge performance of the $Li_{2.90}Na_{0.10}V_2(PO_4)_3/C$ composite.

Fig. 3A shows the V 2p XPS core level of the $Li_{2.90}Na_{0.10}V_2(PO_4)_3/$C composite. The V 2p core level fits to a single peak with a binding
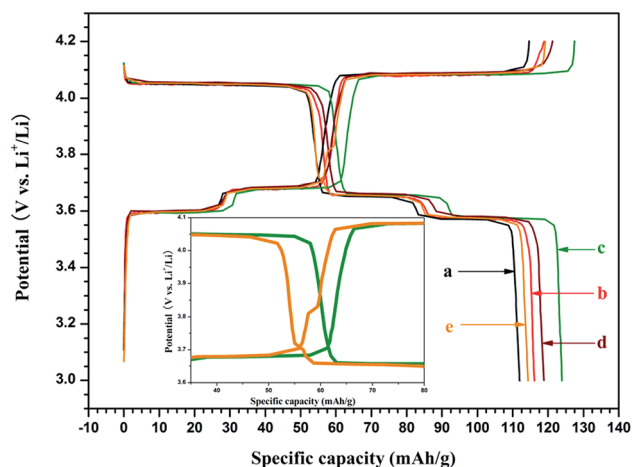
Fig. 2 The initial galvanostatic charge–discharge curves of the $Li_{3-x}Na_xV_2(PO_4)_3/C$ composites. Curves a, b, c, d and e corresponding to $x = 0.04$, 0.06, 0.10, 0.12 and 0.18, respectively.
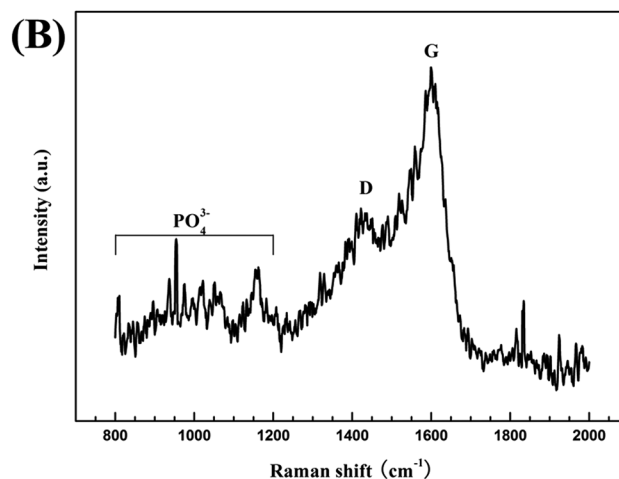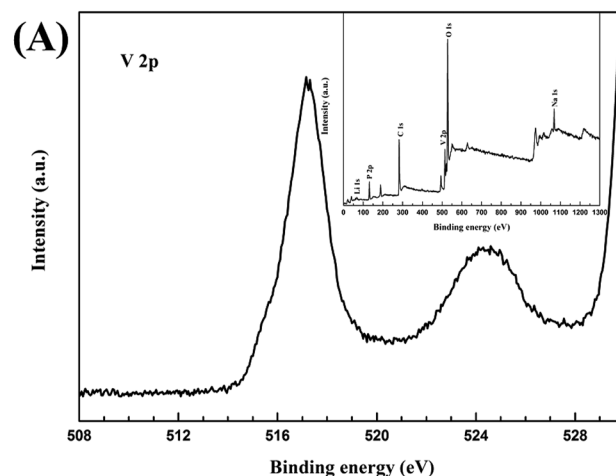
Fig. 3 XPS spectrum of V 2p (A) and Raman spectrum (B) of the $Li_{2.90}Na_{0.10}V_2(PO_4)_3/C$ composite.

energy of 517.3 eV, matching well with the data of V^{3+} in $Li_3V_2(PO_4)_3$ reported in literature (517.2 eV).[10,36] No valance state other than V^{3+} was detected in the $Li_{2.90}Na_{0.10}V_2(PO_4)_3$/C composite, indicating that the constant state of V in the composite is not changed by the Na-doping. The Raman spectrum of the $Li_{2.90}Na_{0.10}V_2(PO_4)_3$/C composite is shown in Fig. 3B, in which the peaks in the range of 800–1200 cm^{-1} correspond to the stretching modes of the $(PO_4)^{3-}$.[39] The peaks in the range of 1550–1660 and 1250–1450 cm^{-1} are assigned to the graphite band (G-band, sp^2 character carbon) and disorder-induced phonon mode (D-band, sp^3 character carbon), respectively. Meanwhile, the I_D/I_G ratio of the $Li_{2.90}Na_{0.10}V_2(PO_4)_3$/C composite calculated from Fig. 3B is *ca.* 0.66, demonstrating that the quality of sp^2 character carbon is much larger than sp^3 character one in the coating carbon. Thus, the coating carbon with much sp^2 characters are beneficial to the electronic conductivity and facilitate the diffusion of Li$^+$. The I_D/I_G ratio of this coating carbon has the similar value as that of the residual carbon which is formation from the frequently used organic carbon precursors, such as PEG, PVA and so on.[35,36] It can be concluded from the present study that the methyl orange used as both Na and carbon sources can form the high-quality carbon matrix which help improving the electron conductivity of the materials without any changes in both the valance state of V and the structure of $Li_{2.90}Na_{0.10}V_2(PO_4)_3$/C composite. Recently, $Li_{3-x}Na_xV_2(PO_4)_3$/C composites can be successfully synthesized after the Na-doping by using different organic carbon precursors and inorganic Na sources,[32–34] but these composites can be only synthesized *via* sol–gel method and rheological phase reaction method attributed to a little volume of Na sources used, which is caused by a low Na-doping level and large bulk density of inorganic Na sources. Based on this, in our work the $Li_{2.90}Na_{0.10}V_2(PO_4)_3$/C

composite can be successful prepared *via* a simple solid-state reaction synthetic route when the methyl orange was chosen as both Na and carbon sources, which is due to the low bulk density of methyl orange compared to that of inorganic salts, and the synthetic route reported here must be the first choice for commercialized produced.

The morphologies of the $Li_{2.90}Na_{0.10}V_2(PO_4)_3$/C composite are shown in Fig. 4, in which the $Li_{2.90}Na_{0.10}V_2(PO_4)_3$/C composite shows primary particle size of *ca.* 80–150 nm with partially agglomeration. HRTEM images (Fig. 4D) shows that the $Li_{2.90}Na_{0.10}V_2(PO_4)_3$ particle is uniformly wrapped by a carbon coating in thickness of *ca.* 4 nm, which has been reported that the *in situ* formed carbon coating plays an important role in suppressing the bulk growth of inorganic particles.[35,36,39,40] Moreover, the carbon coating can help increasing the electronic connecting of the particles and hence enhancing the electronic conductivity of the composite. The electronic conductivity of the $Li_{2.90}Na_{0.10}V_2(PO_4)_3$/C composite measured is about 9.7×10^{-2} S cm^{-1}, which is much higher than that of the $Li_3V_2(PO_4)_3$ (2.3×10^{-8} S cm^{-1}) at 300 K.[11] It is reported that the morphology and specific surface area of the particles have an important influence on the electrochemical performances of $Li_3V_2(PO_4)_3$, so it is necessary to find suitable optimizing particles size or/and introducing conductive additives.[35] As aforementioned that both the highly crystallized structure of Na-doped $Li_{2.90}Na_{0.10}V_2(PO_4)_3$ and the coating carbon with relatively low I_D/I_G ratio were achieved by using methyl orange as both Na and carbon sources. Although $Li_{3-x}Na_xV_2(PO_4)_3$/C composites have been prepared with different inorganic Na sources (Na_2CO_3, $NaNO_3$ and Na_3PO_4) and organic carbon source precursor (citric acid and PEG200) in the previous
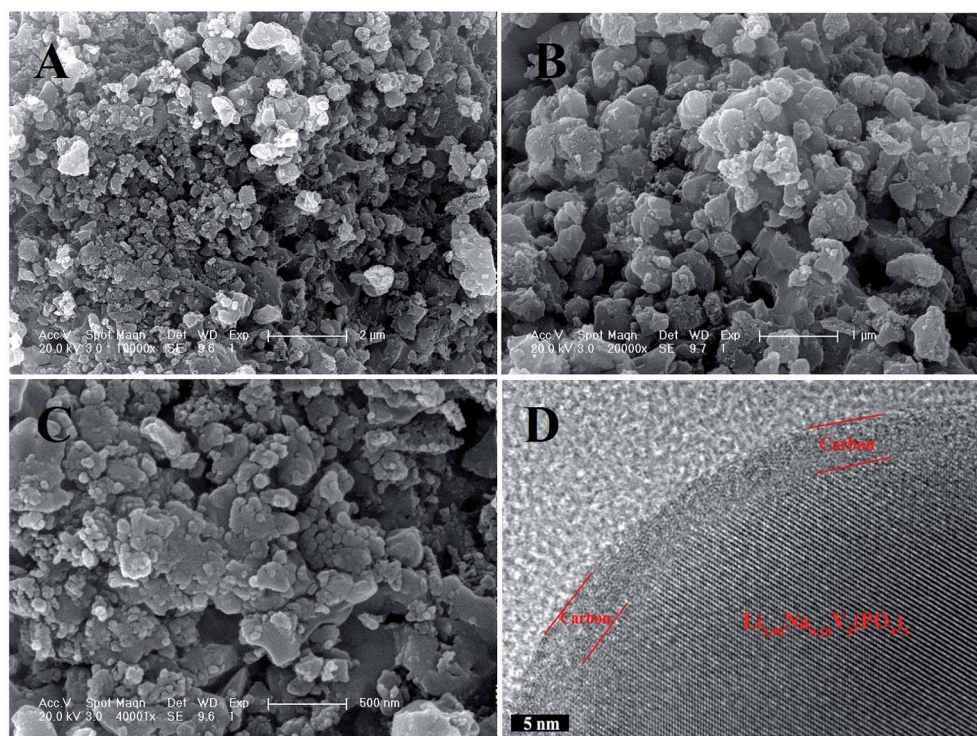

Fig. 4 SEM (A–C) and HRTEM (D) images of the $Li_{2.90}Na_{0.10}V_2(PO_4)_3$/C composite.
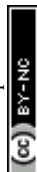
Table 1 The charge/discharge capacity and coulombic efficiency of the $Li_{2.90}Na_{0.10}V_2(PO_4)_3$/C composite at different charge/discharge rates

Charge/discharge rate	0.1C	0.3C	0.5C	1C	2C	5C
The charge capacity (mAh g^{-1})	131	128	121	115	107	99
The discharge capacity (mAh g^{-1})	128	124	118	113	106	98
Columbic efficiency	98%	97%	97%	98%	99%	99%

studies, however, the synthetic routes, which are the sol–gel method[32,33] and rheological phase reaction method,[34] are not suitable for large-scale preparation compared to the solid-state reaction method that is used in this study because of their manufacturing process complexity and time consuming.

3.2 Electrochemical property

Fig. 5A shows the galvanostatic discharge–charge curves of the $Li_{2.90}Na_{0.10}V_2(PO_4)_3$/C composite at different rates with corresponding capacity and coulombic efficiency listed in Table 1. At a low rate of 0.1C, the electrode shows a high discharge specific

capacity of 128 mA h g^{-1} corresponding to 97% of the theoretical specific capacity (132 mA h g^{-1}) for the reversible (de) intercalation of two lithium ions from $Li_3V_2(PO_4)_3$. The $Li_{2.90}Na_{0.10}V_2(PO_4)_3$/C composite exhibits excellent rate capability and coulombic efficiency at high rate. At a high rate of 5C, the capacity of the $Li_{2.90}Na_{0.10}V_2(PO_4)_3$/C composite keeps almost constant within 1100 cycles, as shown in Fig. 5B. The capacity still maintains 95 mA h g^{-1} after 1100 cycles, retaining approximately 97% of the initial capacity and the coulombic efficiency keeps at 100% during the cycling. Fig. 5C displays the specific charge and discharge curves of the $Li_{2.90}Na_{0.10}V_2(PO_4)_3$/C composite and the results are in coincident with Fig. 5B. To our knowledge, only limited cyclic performance (<100 cycles) under moderate rates (≤2C) were reported.[32,33] The promising electrochemical performance of the $Li_{2.90}Na_{0.10}V_2(PO_4)_3$/C composite should be attributed to the enlarged Li$^+$ diffusion channel and the improved electronic conductivity resulted from both the Na-doped and carbon coating, as the larger radius of Na$^+$ than that of the Li$^+$, the diffusion channel of Li$^+$ is likely enlarged after the substitution, which enhances the mobility of lithium ions.[32–34] Without the doping of Na and coating of
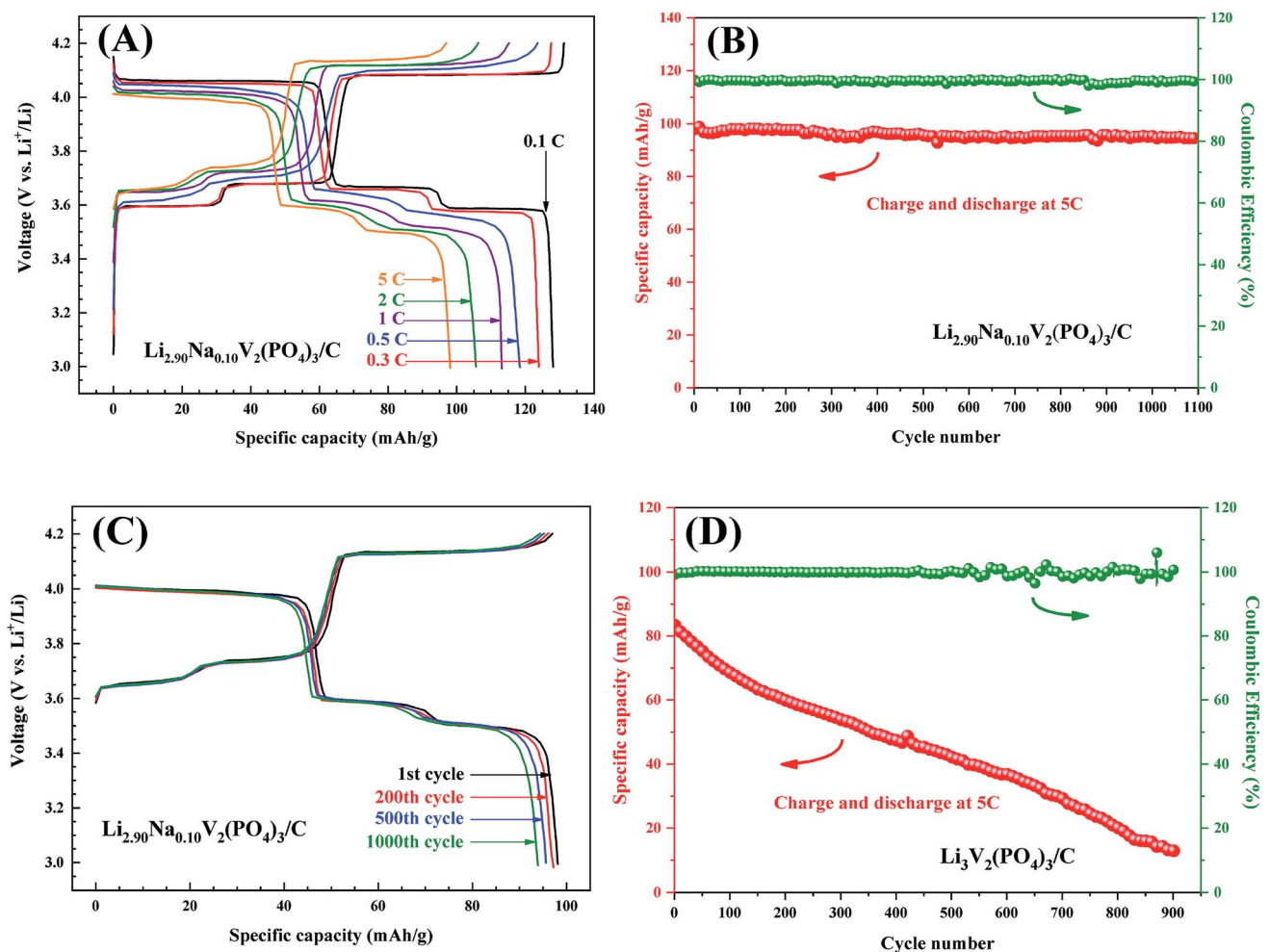

Fig. 5 Initial discharge/charge curves at different rates (A) of the $Li_{2.90}Na_{0.10}V_2(PO_4)_3$/C composite, the cycling performance at 5C (B) and the discharge/charge curves (C) during cycling of the $Li_{2.90}Na_{0.10}V_2(PO_4)_3$/C composite, the cycling performance at 5C (D) of $Li_{3.0}V_2(PO_4)_3$/C composite.

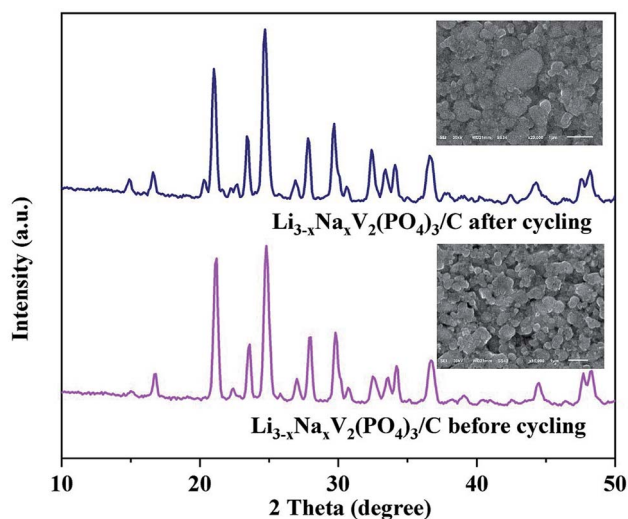**Fig. 6** XRD patterns and SEM images (the inset figures) of the $Li_{2.90}Na_{0.10}V_2(PO_4)_3$/C composite before and after cycling, respectively.

carbon, the cycling performance of $Li_{3.0}V_2(PO_4)_3$ composite at the rate of 5C are poor. The specific capacity of the composite decreases to less than 20 mA h g^{-1} after 900 cycles. By means of the *in situ* introduced carbon, not only nano-particles of $Li_{2.90}Na_{0.10}V_2(PO_4)_3$ are produced, but also the electrical contact between the individual $Li_{2.90}Na_{0.10}V_2(PO_4)_3$ particles is increased, which are beneficial to the cyclic performance of $Li_{2.90}Na_{0.10}V_2(PO_4)_3$/C composite. The (de)intercalation ability of Li$^+$ for $Li_{2.90}Na_{0.10}V_2(PO_4)_3$ is likely enhanced by the Na-doping, which not only enlarges the Li$^+$ diffusion channel, but also enhances the bulk electronic conductivity, and the carbon coating, which also increases the electronic conductivity. In addition, the nano-particles shorten the Li$^+$ diffusion lengths. All the above factors lead to improved electrochemical performances of the $Li_{2.90}Na_{0.10}V_2(PO_4)_3$/C composite, especially the ultrahigh coulombic efficiency at high rates. To further investigate the structure ability of the $Li_{2.90}Na_{0.10}V_2(PO_4)_3$/C composite, the XRD patterns and SEM images of the cathode electrodes after 1000 cycles are acquired as displayed in Fig. 6. It is seen that the peak intensities and positions of the cycled electrodes have limited difference of the result of the electrode before cycling. The SEM images after 1000 cycling also indicates the stability of the $Li_{2.90}Na_{0.10}V_2(PO_4)_3$/C composite.

4. Conclusions

Na-doped $Li_{3-x}Na_xV_2(PO_4)_3$/C (x = 0.04, 0.06, 0.10, 0.12, 0.18) used as cathode for lithium-ion batteries were successfully synthesized *via* a simple carbothermal reduction reaction route by using methyl orange as reduction agent and, Na and carbon sources. Among them, the $Li_{2.90}Na_{0.10}V_2(PO_4)_3$/C composite with a small amount doping of x = 0.10 exhibits excellent rate capability and long-term cyclic stability, in which a specific capacity of 95 mA h g^{-1} is obtained at the current density of 5C after 1100 cycles corresponding to the capacity retention of 97%. The promising electrochemical performance of the $Li_{2.90}Na_{0.10}V_2(PO_4)_3$/C composite is attributed to the synergetic

effect of Na-doping and carbon coating, which supplies enlarged the diffusion channel of Li$^+$ and increased electronic conductivity. As the excellent electrochemical performance of $Li_{2.90}Na_{0.10}V_2(PO_4)_3$/C, and further considering its high safety, it is hopefully that the composite shows a promising candidate as cathode for lithium-ion batteries of hybrid electric vehicles (HEVs) and electric vehicles (EVs) in the future.

Conflicts of interest

There are no conflicts to declare.

Acknowledgements

References

1 J. B. Goodenough, How we made the Li-ion rechargeable battery, *Nat. Electron.*, 2018, **1**, 204.

2 A. K. Padhi, K. S. Nanjundaswamy and J. B. Goodenough, Phospho-olivines as positive-electrode materials for rechargeable lithium batteries, *J. Electrochem. Soc.*, 1997, **144**, 1188–1194.

3 A. K. Padhi, K. S. Nanjundaswamy, C. Masquelier, S. Okada and J. B. Goodenough, Effect of structure on the Fe^{3+}/Fe^{2+} redox couple in iron phosphates, *J. Electrochem. Soc.*, 1997, **144**, 1609–1613.

4 S. Brutti, J. Manzi, A. De Bonis, D. Di Lecce, F. Vitucci, A. Paolone, F. Trequattrini and S. Panero, Controlled synthesis of LiCoPO$_4$ by a solvo-thermal method at 220 C, *Mater. Lett.*, 2015, **145**, 324–327.

5 S. Karthickprabhu, G. Hirankumar, A. Maheswaran, C. Sanjeeviraja and R. S. Daries Bella, Structural and conductivity studies on LiNiPO$_4$ synthesized by the polyol method, *J. Alloys Compd.*, 2013, **548**, 65–69.

6 M. Sato, S. Tajimi, H. Okawa, K. Uematsu and K. Toda, Preparation of iron phosphate cathode material of Li$_3$Fe$_2$(PO$_4$)$_3$ by hydrothermal reaction and thermal decomposition processes, *Solid State Ionics*, 2002, **152–153**, 247–251.

7 A. K. Padhi, K. S. Nanjundaswamy, C. Masquelier and J. B. Goodenough, Mapping of transition metal redox energies in phosphates with NASICON structure by lithium intercalation, *J. Electrochem. Soc.*, 1997, **144**, 2581–2586.

8 S. C. Yin, H. Grondey, P. Strobel, H. Huang and L. F. Nazar, Charge Ordering in Lithium Vanadium Phosphates: Electrode Materials for Lithium-Ion Batteries, *J. Am. Chem. Soc.*, 2003, **125**, 326–327.

9 S. C. Yin, H. Grondey, P. Strobel, M. Anne and L. F. Nazar, Electrochemical property: structure relationships in

monoclinic $Li_{3-y}V_2(PO_4)_3$, *J. Am. Chem. Soc.*, 2003, **125**, 10402–10411.

10 X. H. Rui, Q. Y. Yan, M. Skyllas-Kazacos and T. M. Lim, $Li_3V_2(PO_4)_3$ cathode materials for lithium-ion batteries: a review, *J. Power Sources*, 2014, **285**, 19–38.

11 X. F. Zhang, R. S. Kühnel, H. T. Hu, D. Eder and A. Balducci, Going nano with protic ionic liquids—the synthesis of carbon coated $Li_3V_2(PO4)_3$ nanoparticles encapsulated in a carbon matrix for high power lithium-ion batteries, *Nano Energy*, 2015, **12**, 207–214.

12 Z. Zhang, Y. Han, J. Xu, J. Ma, X. Zhou and J. Bao, Construction of amorphous $FePO_4$ nanosheets with enhanced sodium storage properties, *ACS Appl. Energy Mater.*, 2018, **1**, 4395–4402.

13 E. L. Gu, S. H. Liu, Z. Z. Zhang, Y. Y. Fang, X. S. Zhou and J. C. Bao, An efficient sodium-ion battery consisting of reduced graphene oxide bonded $Na_3V_2(PO_4)(3)$ in a composite carbon network, *J. Alloys Compd.*, 2018, **767**, 131–140.

14 L. Chen, B. Yan, Y. F. Xie, S. M. Wang, X. F. Jiang and G. Yang, Preparation and electrochemical properties of $Li_3V_{1.8}Mn_{0.2}(PO_4)_3$ doped *via* different Mn sources, *J. Power Sources*, 2014, **261**, 188–197.

15 Q. L. Wei, Q. Y. An, D. D. Chen, L. Q. Mai, S. Y. Chen, Y. L. Zhao, K. M. Hercule, L. Xu, A. Minhas-Khan and Q. J. Zhang, One-pot synthesized bicontinuous hierarchical $Li_3V_2(PO_4)_3$/C mesoporous nanowires for high-rate and ultralong-life lithium-ion batteries, *Nano Lett.*, 2014, **14**, 1042–1048.

16 L. L. Zhang, Z. Li, X. L. Yang, X. K. Ding, Y. X. Zhou, H. B. Sun, H. C. Tao, L. Y. Xiong and Y. H. Huang, Binder-free $Li_3V_2(PO_4)_3$/C membrane electrode supported on 3D nitrogen-doped carbon fibers for high-performance lithium-ion batteries, *Nano Energy*, 2017, **34**, 111–119.

17 Y. X. Yang, W. W. Xu, R. S. Guo, L. Liu, S. S. Wang, D. Xie and Y. Z. Wan, Synthesis and electrochemical properties of Zn-doped, carbon coated lithium vanadium phosphate cathode materials for lithium-ion batteries, *J. Power Sources*, 2014, **269**, 15–23.

18 M. M. Ren, M. Z. Yang, W. L. Liu, M. Li, L. W. Su, X. B. Wu and Y. H. Wang, Co-modification of nitrogen-doped graphene and carbon on $Li_3V_2(PO_4)_3$ particles with excellent long-term and high-rate performance for lithium storage, *J. Power Sources*, 2016, **326**, 313–321.

19 X. J. Yang, L. Liu and H. R. Jia, Study on structure and electrochemical performance of Tm^{3+}-doped monoclinic $Li_3V_2(PO_4)_3$/C cathode material for lithium-ion batteries, *Electrochim. Acta*, 2014, **150**, 62–67.

20 W. F. Mao, Y. B. Fu, H. Zhao, G. Ai, Y. L. Dai, D. C. Meng, X. H. Zhang, D. Y. Qu, G. Liu, V. S. Battaglia and Z. Y. Tang, Rational design and facial synthesis of $Li_3V_2(PO_4)_3$@C nanocomposites using carbon with different dimensions for ultrahigh-rate lithium-ion batteries, *ACS Appl. Mater. Interfaces*, 2015, **7**(22), 12057–12066.

21 S. L. Wang, Z. X. Zhang, Z. T. Jiang, A. Deb, L. Yang and S. I. Hirano, Mesoporous $Li_3V_2(PO_4)_3$@CMK-3 nanocomposite cathode material for lithium ion batteries, *J. Power Sources*, 2014, **253**, 294–299.

22 S. L. Wang, Z. X. Zhang, A. Deb, C. C. Yang, L. Yang and S. I. Hirano, Nanostructured $Li_3V_2(PO_4)_3$/C composite as high-rate and long-life cathode material for lithium ion batteries, *Electrochim. Acta*, 2014, **143**, 297–304.

23 Y. Wu, Z. Y. Tang, X. Y. Guo, C. Q. Du and X. H. Zhang, An alginic acid assisted rheological phase synthesis of carbon coated $Li_3V_2(PO_4)_3$ with high-rate performance, *J. Alloys Compd.*, 2014, **616**, 32–41.

24 Q. Z. Ou, Y. Tang, Y. J. Zhong, X. D. Guo, B. H. Zhong, H. Liu and M. Z. Chen, Submicrometer porous $Li_3V_2(PO_4)_3$/C composites with high rate electrochemical performance prepared by sol-gel combustion method, *Electrochim. Acta*, 2014, **137**, 489–496.

25 Y. Z. Luo, X. Xu, Y. X. Zhang, Y. Q. Pi, Y. L. Zhao, X. C. Tian, Q. Y. An, Q. L. Wei and L. Q. Mai, Hierarchical carbon decorated $Li_3V_2(PO_4)_3$ as a bicontinuous cathode with high-rate capability and broad temperature adaptability, *Adv. Energy Mater.*, 2014, **4**, 1400107.

26 X. Y. Cao and J. J. Zhang, Rheological phase synthesis and characterization of $Li_3V_2(PO_4)_3$/C composites as cathode materials for lithium ion batteries, *Electrochim. Acta*, 2014, **129**, 305–311.

27 W. F. Mao, N. N. Zhang, Z. Y. Tang, Y. Q. Feng and C. X. Ma, High rate capability of $Li_3V_2(PO_4)_3$/C composites prepared *via* a TPP-assisted carbothermal method and its application in $Li_3V_2(PO_4)_3||Li_4Ti_5O_{12}$, *J. Alloys Compd.*, 2014, **588**, 25–29.

28 Y. Cheng, W. Zhou, K. Feng, H. Z. Zhang, X. F. Li and H. M. Zhang, One-pot synthesis of 3D hierarchical porous $Li_3V_2(PO_4)(3)$/C nanocomposites for high-rate and long-life lithium ion batteries, *RSC Adv.*, 2017, **7**, 38415–38423.

29 S. Zhang, Q. Wu, C. Deng, F. L. Liu, M. Zhang, F. L. Meng and H. Gao, Synthesis and characterization of Ti-Mn and Ti-Fe codoped $Li_3V_2(PO_4)_3$ as cathode material for lithium ion batteries, *J. Power Sources*, 2012, **218**, 56–64.

30 J. S. Huang, L. Yang, K. Y. Liu and Y. F. Tang, Synthesis and characterization of $Li_3V_{(2-2x/3)}Mg_x(PO_4)_3$/C cathode material for lithium-ion batteries, *J. Power Sources*, 2010, **195**, 5013–5018.

31 C. S. Dai, Z. Y. Chen, H. Z. Jin and X. G. Hu, Synthesis and performance of $Li_3(V_{1-x}Mg_x)_2(PO_4)_3$ cathode materials, *J. Power Sources*, 2010, **195**, 5775–5779.

32 Q. Kuang, Y. M. Zhao and Z. Y. Liang, Synthesis and electrochemical properties of Na-doped $Li_3V_2(PO_4)_3$ cathode materials for Li-ion batteries, *J. Power Sources*, 2011, **196**, 10169–10175.

33 Q. Q. Chen, X. C. Qiao, Y. B. Wang, T. T. Zhang, C. Peng, W. M. Yin and L. Liu, Electrochemical performance of $Li_{3-x}Na_xV_2(PO_4)_3$/C composite cathode materials for lithium ion batteries, *J. Power Sources*, 2012, **201**, 267–273.

34 R. H. Wang, S. H. Xiao, X. H. Li, J. X. Wang, H. J. Guo and F. X. Zhong, Structural and electrochemical performance of Na-doped $Li_3V_2(PO_4)_3$/C cathode materials for lithium-ion batteries *via* rheological phase reaction, *J. Alloys Compd.*, 2013, **575**, 268–272.

35 H. T. Tan, L. H. Xu, H. B. Geng, X. H. Rui, C. C. Li and S. M. Huang, Nanostructured $Li_3V_2(PO_4)_3$ cathodes, *Small*, 2018, **14**, 1800567.

36 J. F. Zhang, H. X. Wei, Y. Cao, C. L. Peng and B. Zhang, Hierarchical $LiMnPO_4 \cdot Li_3V_2(PO_4)_3$/C/rGO nanocomposites as superior-rate and long-life cathodes for lithium ion batteries, *J. Alloys Compd.*, 2018, **769**, 332–339.

37 Z. Y. Wang, W. He, X. D. Zhang, Y. Z. Yue, G. H. Yang, X. L. Yi, Y. Y. Wang and J. C. Wang, $Li_2NaV_2(PO_4)_3$/hard carbon nanocomposite cathodes for high-performance Li- and Na-ion batteries, *ChemElectroChem*, 2017, **4**(3), 671–678.

38 S. Q. Liang, X. X. Cao, Y. P. Wang, Y. Hu, A. Q. Pan and G. Z. Cao, Uniform $8LiFePO_4 \cdot Li_3V_2(PO_4)_3$/C nanoflakes for high-performance Li-ion batteries, *Nano Energy*, 2016, **22**, 48–58.

39 X. L. Wu, L. Y. Jiang, F. F. Cao, Y. G. Guo and L. J. Wan, $LiFePO_4$ nanoparticles embedded in a nanoporous carbon matrix: superior cathode material for electrochemical energy-storage devices, *Adv. Mater.*, 2009, **21**, 2710–2714.

40 H. Liu, F. C. Strobridge, O. J. Borkiewicz, K. M. Wiaderek, K. W. Chapman, P. J. Chupas and C. P. Grey, Capturing metastable structures during high-rate cycling of $LiFePO_4$ nanoparticle electrodes, *Science*, 2017, **344**(6191), 1252817.